Hydrogenolysis of glycerol on bimetallic Pd-Cu/solid-base catalysts prepared via layered double hydroxides precursors

Shuixin Xia [a], Zhenle Yuan [a], Lina Wang [b], Ping Chen [a], Zhaoyin Hou [a,*]

[a] Institute of Catalysis, Department of Chemistry, Zhejiang University, Hangzhou 310028, China
[b] Key Laboratory of Advanced Textile Materials and Manufacturing Technology, Zhejiang Sci-tech University, Hangzhou 310012, China

ARTICLE INFO

ABSTRACT

A series of bimetallic Pd-Cu/solid-base catalysts were prepared via thermal decomposition of $Pd_xCu_{0.4}Mg_{5.6-x}Al_2(OH)_{16}CO_3$ layered double hydroxides precursors and used in hydrogenolysis of glycerol to 1,2-propanediol (1,2-PDO). X-ray diffraction (XRD), scanning electron microscopy (SEM) and N_2O oxidation and followed H_2 titration characterizations confirmed that well structured layered double hydroxides $Pd_xCu_{0.4}Mg_{5.6-x}Al_2(OH)_{16}CO_3$ crystals could be prepared when the amount of added Pd was less than $x < 0.04$. Pd and Cu dispersed highly in reduced $Pd_xCu_{0.4}/Mg_{5.6-x}Al_2O_{8.6-x}$ and Pd improved the reduction of Cu. Hydrogenolysis of glycerol proceeded easily on bimetallic Pd-Cu/solid-base catalysts than separated Pd and Cu. On $Pd_{0.04}Cu_{0.4}/Mg_{5.56}Al_2O_{8.56}$, the conversion of glycerol and selectivity of 1,2-PDO reached 88.0 and 99.6%, respectively, at 2.0 MPa H_2, 180 °C, 10 h in ethanol solution. And this catalyst is stable in five recycles. It was concluded that H_2-spillover from Pd to Cu increased the activity of $Pd_xCu_{0.4}/Mg_{5.6-x}Al_2O_{8.6-x}$ in hydrogenolysis of glycerol.

© 2011 Elsevier B.V. All rights reserved.

1. Introduction

Recently, there is an increasing interesting on using biodiesel as an alternative fuel [1,2]. The rapid rising production of biodiesel has led to a drastic surplus of glycerol [2]. Many biodiesel production factories now view crude glycerol as a waste. Many efforts have been reported on the conversion of glycerol into value-added products, such as catalytic oxidation of glycerol to glyceric acid [3–6] and dihydroxyacetone [4–6], dehydration of glycerol to acrolein [7–10] and hydrogenolysis of glycerol to propanediols [11–16]. Among these reported technologies, catalytic synthesis of propanediols from glycerol instead of the expensive hydration of petro-based propylene oxide is more favorable in green chemistry and industrial application [2,11–24].

In published papers, hybrid $Rh/C + H_2WO_4$ [12], Ru/C (or Rh/SiO_2) + Amberlyst [13,14], $Pt/SiO_2–Al_2O_3$ [11] and ruthenium-doped acidic heteropoly salt $Cs_{2.5}H_{0.5}[PW_{12}O_{40}]$ were studied in detail in hydrogenolysis of glycerol to propanediols. It was suggested that glycerol hydrogenolysis performed in consecutive glycerol dehydration to acetol (on acid sites) and acetol hydrogenation to propanediols (on metal particles) in acidic conditions (see Scheme 1) [25–43]. But the conversion of glycerol was low and mainly noble metals were reported in acidic conditions. On the other hand, it was reported that NaOH can accelerate the conver-

sion of glycerol in combined Pt/C + NaOH [31,32], Ru/TiO_2 + NaOH [44] and Cu/ZnO + NaOH [45] catalytic solutions. It was deduced that glycerol hydrogenolysis proceeded in a distinct dehydrogenation–dehydration–hydrogenation mechanism in base solutions (see Scheme 2) [31–42]. But NaOH also catalyzed the cleavage of C–C bond and increased the formation of undesired products like ethylene glycol, ethanol and methanol [31,32]. And the addition of NaOH inevitably resulted in other drawbacks such as the reaction mixture needs further neutralization and environmental pollution.

According to these mechanisms, we thought that a solid bifunctional catalyst consisting of both metal and acid/base sites should be capable for this reaction. Choosing solid-base and/or solid-acid as a co-catalyst and support would be a good substitute for the reported hybrid catalysts. Because crude glycerol derived from biodiesel production contains a variety of impurities (such as unreacted catalysts, NaOH or other alkali metal hydroxides) and these contaminants are poisons to solid-acid [33–35], solid-base should be a good co-catalyst and support in industrial application.

In our previous works, hydrotalcite, MgO, Al_2O_3, HZSM-5 and H-Beta supported Pt catalysts were first tested in hydrogenolysis of glycerol. It was found that solid-base (such as hydrotalcite and MgO) supported Pt catalysts exhibited predominant activity and higher 1,2-propanediol (1,2-PDO) selectivity than that of solid acids (Al_2O_3, H-ZSM-5 and H-Beta) [36]. And MgO supported copper is also active in this reaction [37]. More recently, we found that a homogenously dispersed copper on layered solid-base catalyst is more effective in the hydrogenolysis of glycerol in aqueous solution. The best yield of 1,2-PDO reached 78.5% at 180 °C, 3.0 MPa

* Corresponding author. Tel.: +86 571 88273283; fax: +86 571 88273283.
E-mail address: zyhou@zju.edu.cn (Z. Hou).
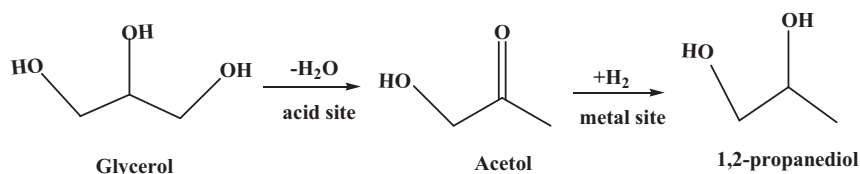
Scheme 1. Glycerol hydrogenolysis in acidic conditions.
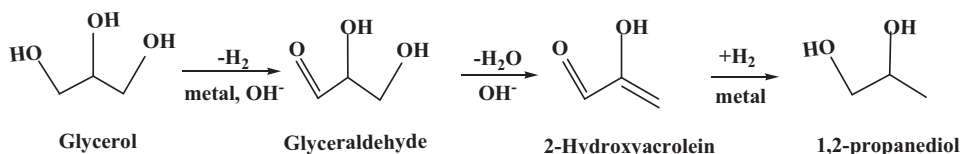
Scheme 2. Glycerol hydrogenolysis in base solutions.

H_2 and 20 h [38]. In these works, it was disclosed that the activity of bi-functional Cu/solid-base catalysts increased with the alkali strength of solid-base. However, the influence of active metals (hydrogenation center in Scheme 2) in bi-functional metal/solid-base catalysts has not been specified.

In this work, a series of bimetallic Pd-Cu/solid-base catalysts were prepared via thermal decomposition of $Pd_xCu_{0.4}Mg_{5.6-x}Al_2(OH)_{16}CO_3$ layered double hydroxides precursors. And these catalysts were used in hydrogenolysis of glycerol to 1,2-PDO in different solvents at low hydrogen pressure (2.0 MPa) and short time (10 h). These catalysts were characterized by N_2-adsorption, X-ray diffraction (XRD), scanning electron microscopy (SEM), temperature-programmed reduction with H_2 (H_2-TPR) and N_2O oxidation and followed H_2 titration. The structure–property relationships of these bimetallic Pd-Cu/solid-base catalysts in hydrogenolysis of glycerol to 1,2-PDO were discussed.

2. Experimental

2.1. Catalyst preparation

A series of Pd-containing $Pd_xCu_{0.4}Mg_{5.6-x}Al_2(OH)_{16}CO_3$ layered double hydroxides precursors were first prepared by coprecipitation. Calculated amount of $PdCl_2$, $Cu(NO_3)_2\cdot3H_2O$, $Al(NO_3)_3\cdot9H_2O$ and $Mg(NO_3)_2\cdot6H_2O$ (AR, Shanghai Chemicals, China) were dissolved together in 400 mL deionized water, which was referred as solution A. Solution B was the mixture of Na_2CO_3 and NaOH (AR, Shanghai Chemicals, China) with concentration of 0.25 and 0.8 mol/L, respectively. Solutions A and B were simultaneously added into a glass reactor under vigorous stirring at room temperature and a pH value of 9.5. The slurry was aged at 120 °C for 20 h, filtered off, and washed thoroughly with distilled water until free of Cl⁻. The precipitate was then dried at 80 °C overnight and identified as $Pd_xCu_{0.4}Mg_{5.6-x}Al_2(OH)_{16}CO_3$, in which x referred to amount of added Pd. The layered double structure of prepared $Pd_xCu_{0.4}Mg_{5.6-x}Al_2(OH)_{16}CO_3$ sample was confirmed by XRD (see Fig. 1).

Secondly, these Pd-containing layered double hydroxides were calcined at 400 °C in a stationary air for 4 h and the product catalysts were identified as $Pd_xCu_{0.4}Mg_{5.6-x}Al_2O_9$ and used for characterization. After hydrogen reduction at 300 °C for 1 h, these catalysts were identified as $Pd_xCu_{0.4}/Mg_{5.6-x}Al_2O_{8.6-x}$, in which x referred to amount of added Pd.

2.2. Characterizations

Actual composition of the prepared $Pd_xCu_{0.4}Mg_{5.6-x}Al_2(OH)_{16}CO_3$ precursors was checked and confirmed by inductively coupled plasma-atomic emission spectroscopy (ICP, plasma-Spec-II spectrometer). Samples were first dissolved with aqua regia, and the mixtures were further oxidized with 30% hydrogen peroxide in order to make Pd dissolved completely. N_2 adsorption was measured at its normal boiling point using an ASAP 2010 analyzer (Micromeritics) after pretreated at 250 °C for 4 h in vacuum. BET surface area and BJH pore size distribution were calculated using their desorption isotherms. XRD patterns were detected at room temperature on a Rigaku D/WAX-2500 diffractometer using Cu Kα radiation (λ = 1.5406 Å) with a 2θ step of 0.02°. SEM images of these hydrotalcite-like samples were taken on a microscope (Leo Series VP 1430, Germany) having silicon detector equipped with energy-dispersive X-ray (EDX) facility (Oxford instruments). Samples were coated with gold using sputter coating to avoid charging. Analysis was carried out at an accelerating voltage of 15 kV. H_2-TPR studies were carried out in a quartz reactor. Samples were first pretreated at 450 °C for 1 h under N_2 at a flow rate of 30 mL/min and cooled to room temperature. A reduction agent (10% H_2/N_2 mixture, 30 mL/min) was shifted and the reactor was heated to 450 °C at a ramp of 10 °C/min. Effluent gas was dried by powder KOH and the consumption of hydrogen
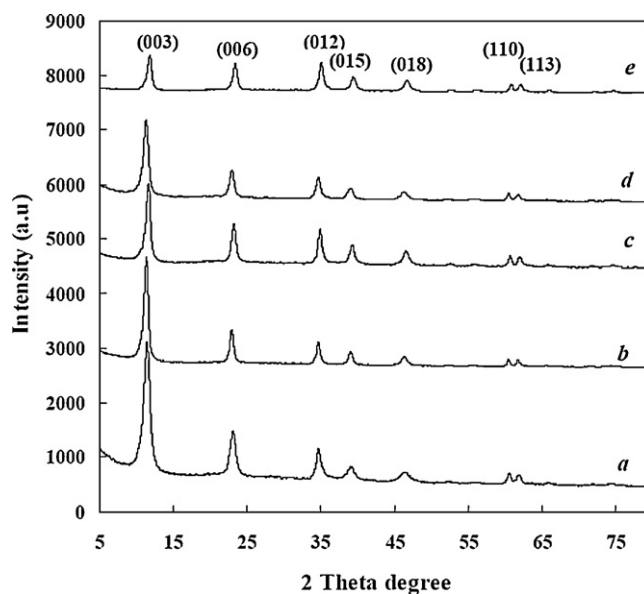

Fig. 1. XRD patterns of fresh $Pd_xCu_{0.4}Mg_{5.6-x}Al_2(OH)_{16}CO_3$ LDHs. (a) $Cu_{0.4}Mg_{5.6}Al_2(OH)_{16}CO_3$; (b) $Pd_{0.008}Cu_{0.4}Mg_{5.592}Al_2(OH)_{16}CO_3$; (c) $Pd_{0.024}Cu_{0.4}Mg_{5.576}Al_2(OH)_{16}CO_3$; (d) $Pd_{0.04}Cu_{0.4}Mg_{5.56}Al_2(OH)_{16}CO_3$; (e) $Pd_{0.08}Cu_{0.4}Mg_{5.52}Al_2(OH)_{16}CO_3$.

Table 1
The structure of the calcined catalysts and Cu dispersion in reduced catalyst.

Catalyst	Crystallite size (nm)[a]		Structure[a]			Cu dispersion[b]		
	MgO	CuO	Pore volume (cm³/g)	Pore size (nm)	S_{BET} (m²/g)	Dispersion[b] (%)[c]	Cu surface area[b] (m²/g Cu)	Cu particle size[b] (nm)
$Cu_{0.4}Mg_{5.6}Al_2O_9$	3.9	2.7	0.860	16.8	204.6	43.2 (±6%)	584.5	2.3
$Pd_{0.008}Cu_{0.4}Mg_{5.592}Al_2O_9$	3.6	1.8	–	–	176.0	58.7 (±6%)	794.2	1.7
$Pd_{0.024}Cu_{0.4}Mg_{5.576}Al_2O_9$	3.7	3.9	–	–	158.2	32.3 (±6%)	437.0	3.1
$Pd_{0.04}Cu_{0.4}Mg_{5.56}Al_2O_9$	4.2	2.6	0.436	14.2	145.1	46.0 (±6%)	622.4	2.2
$Pd_{0.08}Cu_{0.4}Mg_{5.52}Al_2O_9$	5.7	5.3	0.601	15.5	154.8	21.4 (±6%)	289.5	4.7

[a] All of the catalysts are calcined at 400 °C, 4 h.
[b] Calculated from N_2O chemical adsorption after the catalysts were reduced in H_2 at 400 °C.
[c] Data in parentheses are estimated standard deviation that were calculated on the deviation of H_2 consumption in repeated TPR experiments.

were recorded by thermal conductivity detector (TCD). Calibration of the instrument was carried out with CuO of known amount. The number of surface metallic copper sites was determined by N_2O oxidation and followed H_2 titration using the procedure described by Van Der Grift et al. [46], Gervasini and Bennici [47]. Catalysts were first reduced in the procedure described in above TPR experiment in 10% H_2/N_2 mixture at a flow rate of 30 mL/min until 450 °C. The amount of hydrogen consumption in the first TPR was denoted as X. And then the reactor was purged with He to 50 °C. 20% N_2O/N_2 (30 mL/min) was shifted to oxidize surface copper atoms to Cu_2O at 50 °C for 0.5 h. The reactor was flushed with He to remove the oxidant. Finally, another TPR experiment was performed in 10% H_2/N_2, 10 °C/min at a flow rate of 30 mL/min. Hydrogen consumption in the second TPR was denoted as Y. The dispersion of Cu and exposed Cu surface area were calculated according to the equations reported by Van Der Grift et al. [46], which are shown below:

Reduction of all copper atoms:

$$CuO + H_2 \rightarrow Cu + H_2O, \text{ hydrogen consumption in the first TPR } = X$$

Reduction of surface copper atoms only:

$$Cu_2O + H_2 \rightarrow 2Cu + H_2O, \text{ hydrogen consumption in this TPR } = Y$$

And the dispersion of Cu and exposed Cu surface area were calculated as:

$$D = \frac{2Y}{X} \times 100\%$$

$$S = \frac{2Y \times N_{av}}{X \times M_{Cu} \times 1.4 \times 10^{19}} = \frac{1353Y}{X}(\text{m}^2\text{-Cu/g-Cu})$$

where N_{av} is the Avogadro's constant, M_{Cu} is the relative atomic mass (63.456 g/mol), 1.4×10^{19} comes from that an equal abundance of an average copper surface atom area of 0.0711 nm^2, equivalent to 1.4×10^{19} copper atoms/m².

Average volume-surface diameter can be expressed as a function:

$$d_{v.s.} = \frac{6}{(S \times \rho_{Cu})} \approx 0.5\frac{X}{Y}(\text{nm})$$

where, ρ_{Cu} is the density of copper (8.92 g/cm³).

The structure of the reduced catalysts was further detected by XRD and transmission electron microscopy (TEM). Before analysis, catalysts were reduced in a stream of H_2 at 300 °C for 1 h; the reduced powders were poured into alcohol under the protection of H_2. In TEM analysis, the reduced samples were suspended in alcohol with an ultrasonic dispersion for 10 min, and then the resulted solution was dropped on carbon film of nickel grid.
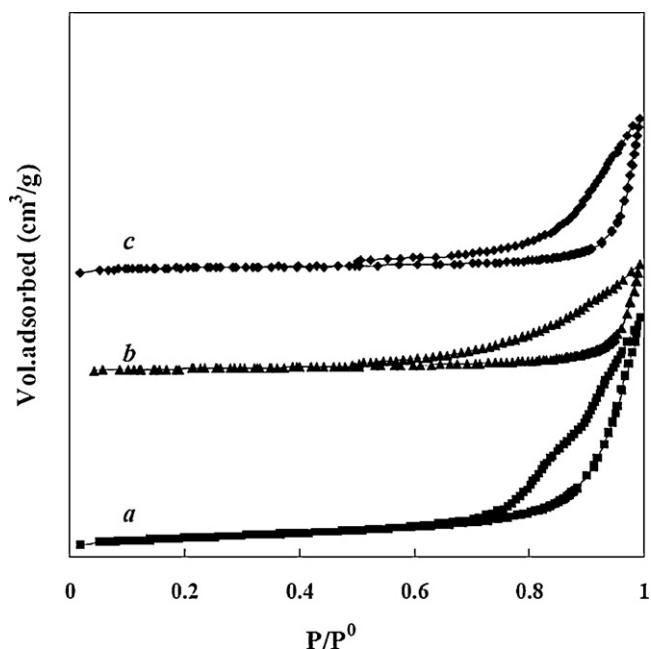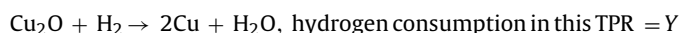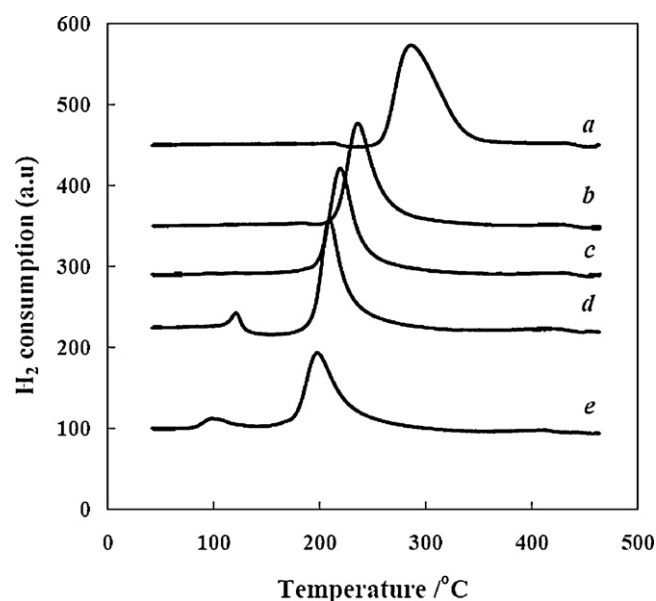

Fig. 2. N_2 adsorption isotherms at −196 °C. (a) $Cu_{0.4}Mg_{5.6}Al_2O_9$; (b) $Pd_{0.04}Cu_{0.4}Mg_{5.56}Al_2O_9$; (c) $Pd_{0.08}Cu_{0.4}Mg_{5.52}Al_2O_9$.

Fig. 3. H_2-TPR profiles of calcined samples. (a) $Cu_{0.4}Mg_{5.6}Al_2O_9$; (b) $Pd_{0.008}Cu_{0.4}Mg_{5.592}Al_2O_9$; (c) $Pd_{0.024}Cu_{0.4}Mg_{5.576}Al_2O_9$; (d) $Pd_{0.04}Cu_{0.4}Mg_{5.56}Al_2O_9$; (e) $Pd_{0.08}Cu_{0.4}Mg_{5.52}Al_2O_9$.
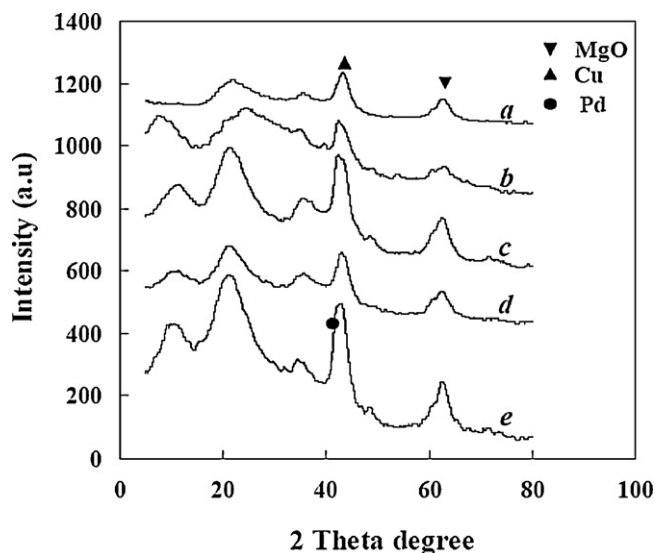
Fig. 4. XRD patterns of the reduced catalysts. (a) $Cu_{0.4}/Mg_{5.6}Al_2O_{8.6}$; (b) $Pd_{0.008}Cu_{0.4}/Mg_{5.592}Al_2O_{8.592}$; (c) $Pd_{0.024}Cu_{0.4}/Mg_{5.576}Al_2O_{8.576}$; (d) $Pd_{0.04}Cu_{0.4}/Mg_{5.56}Al_2O_{8.56}$; (e) $Pd_{0.08}Cu_{0.4}/Mg_{5.52}Al_2O_{8.52}$.

The acidity, alkalinity and H_2 activation activity of reduced catalysts were carried out via temperature-programmed desorption of NH_3, CO_2 and H_2 (NH_3-TPD, CO_2-TPD and H_2-TPD). Sample was first reduced at 300 °C in H_2 flow of 30 mL/min for 1 h, purged by purified Ar and further treated at 450 °C for 0.5 h in Ar. And then the reactor was cooled to 50 °C in Ar, exposed to 20% NH_3/Ar (or 20% CO_2/Ar or 10% H_2/Ar) for 30 min, purged by Ar for 5 h at 50 °C in order to eliminate the physical adsorbed NH_3 (or CO_2 or H_2). Temperature-programmed desorption was conducted by ramping to 550 °C at 10 °C/min and NH_3 ($m/e = 16$) (or CO_2 ($m/e = 44$) or H_2 ($m/e = 2$)) in effluent was detected and recorded as a function of temperature by a quadrupole mass spectrometer (OmniStarTM, GSD301, Switzerland).

2.3. Catalytic reactions

Hydrogenolysis of glycerol was performed in a custom-designed 50 mL stainless steel autoclave equipped with a thermoelectric couple. Before reaction, catalyst was pretreated in a stream of H_2 at 300 °C for 1 h. The reaction mixture included 8.0 g aqueous solution of glycerol (75 wt%) and 1.0 g reduced catalyst. Then the autoclave was purged with H_2 to 2.0 MPa and placed in an oil bath preheated to required temperature and maintained at that temperature for a given time under vigorously stirring with a magnetic stirrer (MAG-NEO, RV-06M, Japan). After reaction, the reactor was cooled to room temperature. Vapor phase was collected by a gas-bag and analyzed with a gas chromatograph (Shimadzu, 8 A) with TCD detector, liquid phase was centrifuged to remove solid catalyst powder and analyzed using a FID gas chromatograph (Shimadzu, 14 B) equipped with a 30 m capillary column (DB-WAX 52 CB, USA). All products detected in liquid were verified by a GC–MS system (Agilent 6890) and quantified via external calibration method. The selectivity of products was calculated on carbon basis.

3. Results and discussion

3.1. X-ray diffraction

Fig. 1 shows the XRD patterns of $Pd_xCu_{0.4}Mg_{5.6-x}Al_2(OH)_{16}CO_3$ precursors dried at 80 °C. All samples had the characteristic reflections of layered double hydroxides. No diffraction peak of separated

Pd-containing oxide or Cu-containing oxide was observed. Sharp and symmetrical reflections at 11.7, 23.2, 60.6 and 61.8° are designated to diffraction of (0 0 3), (0 0 6), (1 1 0) and (1 1 3) plane in layered structure. All characteristic reflection peaks of a well-crystallized hydrotalcite (JCPDS 41-1428) were detected. But the intensity of (0 0 3) reflection decreased with the amount of added Pd, which means that the orderliness of layered double hydroxide crystallite declined at high Pd content. This decline could be ascribed to the ionic radii of Pd^{2+} ion (0.64 Å) is smaller than that of Mg^{2+} ion (0.72 Å) and Cu^{2+} ion (0.73 Å) [48]. SEM images of the $Pd_xCu_{0.4}Mg_{5.6-x}Al_2(OH)_{16}CO_3$ precursors also confirmed that the orderliness of these layered double hydrotalcite crystals decreased with increasing amount of added Pd (see Fig. S1 in the supplementary data). The average thickness of solid lamellar is around 20 nm in $Cu_{0.4}Mg_{5.6}Al_2(OH)_{16}CO_3$ (Fig. S1A), and this thickness decreased to 14–15 nm in $Pd_{0.008}Cu_{0.4}Mg_{5.592}Al_2(OH)_{16}CO_3$ (Fig. S1B) and $Pd_{0.04}Cu_{0.4}Mg_{5.56}Al_2(OH)_{16}CO_3$ (Fig. S1C), and further decreased to 10 nm in $Pd_{0.08}Cu_{0.4}Mg_{5.52}Al_2(OH)_{16}CO_3$ (Fig. S1D).

After calcination at 400 °C for 4 h, separated CuO and MgO were detected in the calcined $Pd_xCu_{0.4}Mg_{5.6-x}Al_2O_9$ catalyst (see Fig. S2 in the supplementary data), and the calculated crystallite sizes of CuO and MgO were summarized in Table 1.

3.2. N2-adsorption

Nitrogen adsorption–desorption isotherms of calcined $Cu_{0.4}Mg_{5.6}Al_2O_9$, $Pd_{0.04}Cu_{0.4}Mg_{5.56}Al_2O_9$ and $Pd_{0.08}Cu_{0.4}Mg_{5.52}Al_2O_9$ are shown in Fig. 2. All of them are type IV pattern according to the IUPAC classification. The closure points of hysteresis loops of $Cu_{0.4}Mg_{5.6}Al_2O_9$ located at a relative pressure of 0.6. However, the hysteresis loops of $Pd_{0.04}Cu_{0.4}Mg_{5.56}Al_2O_9$ and $Pd_{0.08}Cu_{0.4}Mg_{5.52}Al_2O_9$ closed at 0.5, which suggested that the pore diameter decreased with the amount of added Pd. The calculated pore diameter of $Cu_{0.4}Mg_{5.6}Al_2O_9$, $Pd_{0.04}Cu_{0.4}Mg_{5.56}Al_2O_9$ and $Pd_{0.08}Cu_{0.4}Mg_{5.52}Al_2O_9$ were 16.8, 14.2, 15.5 nm, respectively. The calculated BET surface area of these catalysts decreased continuously from 204.6 m²/g (of $Cu_{0.4}Mg_{5.6}Al_2O_9$) to 154.8 m²/g (of $Pd_{0.08}Cu_{0.4}Mg_{5.52}Al_2O_9$) with increasing amount of added Pd (Table 1). These decreases in pore diameter and surface area could also be ascribed to that the orderliness of layered double hydrotalcite $Pd_xCu_{0.4}Mg_{5.6-x}Al_2(OH)_{16}CO_3$ precursors declined with increasing amount of added Pd (see Fig. 1).

3.3. H2-TPR

Fig. 3 shows the H_2-TPR profiles of calcined $Cu_{0.4}Mg_{5.6}Al_2O_9$ and $Pd_xCu_{0.4}Mg_{5.6-x}Al_2O_9$. Only one broader peak from 250 to 340 °C was detected in $Cu_{0.4}Mg_{5.6}Al_2O_9$. This hydrogen consumption could be designated to the reduction of Cu^{2+} ions in lamellar structure of $Cu_{0.4}Mg_{5.6}Al_2O_9$ [38]. And this reduction temperature is higher than that of $Cu_{0.4}Mg_{5.6}Al_2O_9$ prepared at 300 °C [38], which indicated that Cu species in $Cu_{0.4}Mg_{5.6}Al_2O_9$ catalyst pretreated at higher calcination temperature are more stable. It is quite interesting to find that the reduction peak of copper dropped obviously to 220–270 °C in $Pd_{0.008}Cu_{0.4}Mg_{5.592}Al_2O_9$. And then the reduction peak dropped continuously to lower temperature with the increasing amount of added Pd. Another separated peak (at 100–120 °C) appeared when added amount of Pd increased to $x > 0.04$, this hydrogen consumption could be designated to the reduction of Pd^{2+} ions to Pd in lamellar structure of $Pd_xCu_{0.4}Mg_{5.6-x}Al_2O_9$ [49–52]. At the same time, it can be found that the hydrogen consumption peak became sharp and narrow with the increasing amount of added Pd. These results indicated that the reducibility of Cu^{2+} ions in lamellar structure of $Pd_xCu_{0.4}Mg_{5.6-x}Al_2O_9$ was improved obviously by Pd. This improvement could be ascribed to that hydrogen is easily dissociated on Pd and then spills over to Cu^{2+} ions. That is, the
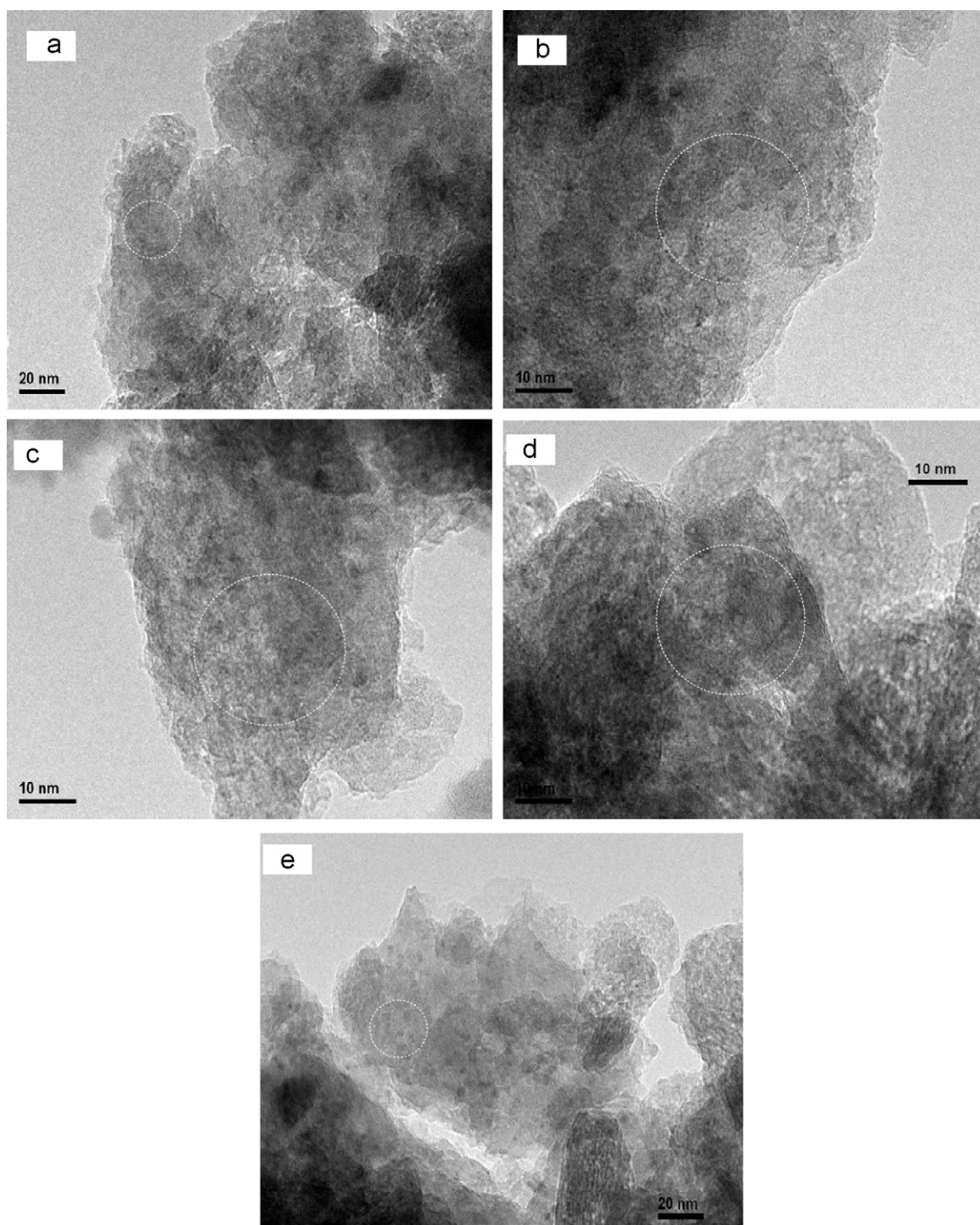
Fig. 5. TEM images of the reduced catalysts. (a) $Cu_{0.4}/Mg_{5.6}Al_2O_{8.6}$; (b) $Pd_{0.008}Cu_{0.4}/Mg_{5.592}Al_2O_{8.592}$; (c) $Pd_{0.024}Cu_{0.4}/Mg_{5.576}Al_2O_{8.576}$; (d) $Pd_{0.04}Cu_{0.4}/Mg_{5.56}Al_2O_{8.56}$; (e) $Pd_{0.08}Cu_{0.4}/Mg_{5.52}Al_2O_{8.52}$.

addition of Pd in $Pd_xCu_{0.4}Mg_{5.6-x}Al_2O_9$ could provide a high concentration of active hydrogen that is susceptible for use in Cu^{2+} ions reduction. The ratio between the amount of hydrogen consumed and the amount of reducible species (Cu^{2+} and Pd^{2+}) was determined quantitatively. It was found that the calculated H_2/M ratio increased from 1.06 (of $Pd_{0.008}Cu_{0.4}Mg_{5.592}Al_2O_9$) to 1.14 (of $Pd_{0.08}Cu_{0.4}Mg_{5.52}Al_2O_9$). These results could be attributed to that active hydrogen formed on the surface of Pd would spillover to the surface of Cu and catalyst support [49–52]. That is, part amount of

dissociated hydrogen would store on the surface of Cu and support materials.

3.4. N_2O oxidation and followed H_2 titration

N_2O oxidation and followed H_2 titration experiments were carried out in order to identify the dispersion of copper. Copper dispersion, exposed copper area and average volume-surface diameter were calculated by these equations reported by Van Der

Grift et al. [46]. These results were summarized in Table 1. It can be found that the dispersion, exposed area and average diameter of copper in reduced $Cu_{0.4}/Mg_{5.6}Al_2O_{8.6}$ (calcined at 400 °C) are 43.2%, 584.5 m^2/g-Cu and 2.3 nm. Small amount of Pd ($x < 0.04$) improved the dispersion of Cu in $Pd_xCu_{0.4}/Mg_{5.6-x}Al_2O_{8.6-x}$ slightly. And the detected dispersion and exposed area of copper in reduced $Pd_{0.04}Cu_{0.4}/Mg_{5.56}Al_2O_{8.56}$ increased to 46.0% and 622.4 m^2/g-Cu. But high amount of Pd decreased the dispersion of copper. These values are generally in agreement with that obtained in XRD and N_2-adsorption because the orderliness of $Pd_{0.08}Cu_{0.4}Mg_{5.52}Al_2(OH)_{16}CO_3$ precursors and the surface area of calcined $Pd_{0.08}Cu_{0.4}/Mg_{5.52}Al_2O_{8.52}$ decreased obviously.

3.5. XRD analysis and TEM images of the reduced catalysts

XRD analysis of the reduced $Pd_xCu_{0.4}/Mg_{5.6-x}Al_2O_{8.6-x}$ catalysts was shown in Fig. 4. It can be found that the diffraction lines of layered double hydrotalcite disappeared after hydrogen reduction and separated Cu (JCPDS 04-0836) and MgO (JCPDS 45-0946) were detected at 43.7 and 63.5°, respectively. The calculated crystalline size of Cu changed in the same sequence as that detected in N_2O oxidation and followed H_2 titration (see Table 1). No diffraction line of Pd was detected in $Pd_xCu_{0.4}/Mg_{5.6-x}Al_2O_{8.6-x}$ catalysts when the added amount of Pd was less than $x < 0.4$, which could be attributed to that Pd dispersed highly and/or the added amount of Pd is low. But a faint diffraction line of Pd (JCPDS 46-1043) might appear in $Pd_{0.08}Cu_{0.4}/Mg_{5.52}Al_2O_{8.52}$ at around 40°, which just overlapped with the diffraction peak of Cu. This result means that separated Pd particles would form because the added amount of Pd is high and/or the surface area of this sample is low (154.8 m^2/g).

The highly dispersion state of Cu and Pd in the reduced $Pd_xCu_{0.4}/Mg_{5.6-x}Al_2O_{8.6-x}$ catalysts were also confirmed by TEM analysis (Fig. 5). No separated Cu particle was detected in the samples. EDX analysis of these samples (denoted in the dashed circle) confirmed that the surface compositions of these catalysts are similar as their bulk content (see Fig. S3 in supplementary data). On the other hand, separated Pd particles (sized in 1.5–2.2 nm) appeared in the TEM images of $Pd_{0.08}Cu_{0.4}/Mg_{5.52}Al_2O_{8.52}$ (Fig. 5e). These results are similar as that detected in N_2O oxidation and followed H_2 titration and XRD analysis. The formation of separated of Pd particles in $Pd_{0.08}Cu_{0.4}/Mg_{5.52}Al_2O_{8.52}$ could be attributed to that the crystalline structure of $Pd_{0.08}Cu_{0.4}Mg_{5.52}Al_2(OH)_{16}CO_3$ is poor, the surface area of calcined $Pd_{0.08}Cu_{0.4}Mg_{5.52}Al_2O_9$ is low and the content of Pd is the highest.

3.6. The acidity and basicity of the reduced $Pd_xCu_{0.4}/Mg_{5.6-x}Al_2O_{8.6-x}$

The acidity of reduced $Pd_xCu_{0.4}/Mg_{5.6-x}Al_2O_{8.6-x}$ catalysts were detected via NH_3-TPD and shown in Fig. 6A. It can be found that mainly one desorption peak was detected in the temperature ranged in 140–290 °C and the amount of desorbed NH_3 decreased slightly with the added amount of Pd. The detected amount of desorbed NH_3 decreased in the same sequence as their surface area (see Table 1). These results indicated that only one kind of very weak acid site existed on the surface of $Pd_xCu_{0.4}/Mg_{5.6-x}Al_2O_{8.6-x}$ catalysts, the acidity is weak and the total amount of acid site is low [53–56].

CO_2-TPD profile of reduced $Pd_xCu_{0.4}/Mg_{5.6-x}Al_2O_{8.6-x}$ catalysts are shown in Fig. 6B. The desorption profile of CO_2 in effluent can be deconvoluted into a main peak (at 145 °C) and a shoulder peak at 360 °C. The first peak could be assigned to desorption of CO_2 on the surface of catalysts, and its amount also decreased with the added amount of Pd. The second peak could be assigned to the basic

sites of the MgO containing catalysts [38]. But the total amount of desorbed CO_2 changed slightly.

3.7. H_2-TPD

The hydrogen activation and its spillover ability over $Pd_xCu_{0.4}/Mg_{5.6-x}Al_2O_{8.6-x}$ catalysts were tested by H_2-TPD and shown in Fig. 7. It can be found that no desorption peak was observed in the whole T range over $Cu_{0.4}/Mg_{5.6}Al_2O_{8.6}$. However,
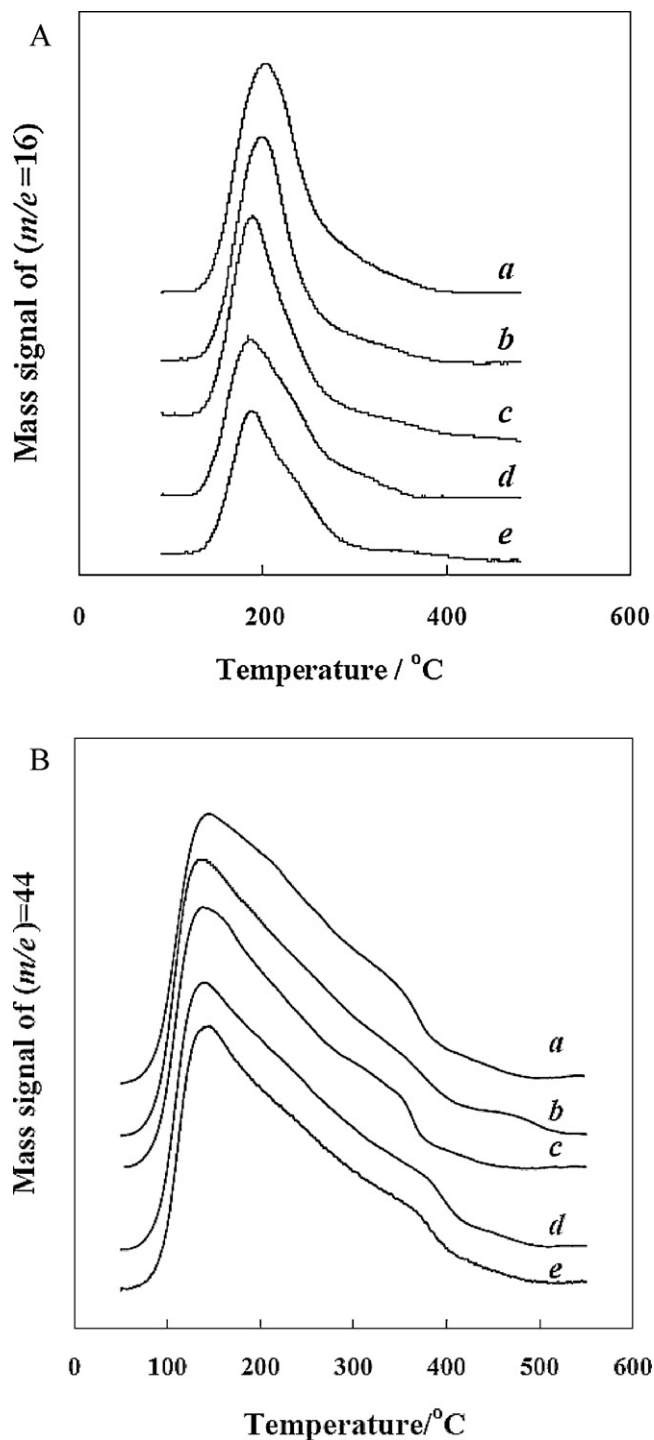
Fig. 6. NH_3-TPD (A) and CO_2-TPD (B) profiles of the reduced catalysts. (a) $Cu_{0.4}/Mg_{5.6}Al_2O_{8.6}$; (b) $Pd_{0.008}Cu_{0.4}/Mg_{5.592}Al_2O_{8.592}$; (c) $Pd_{0.024}Cu_{0.4}/Mg_{5.576}Al_2O_{8.576}$; (d) $Pd_{0.04}Cu_{0.4}/Mg_{5.56}Al_2O_{8.56}$; (e) $Pd_{0.08}Cu_{0.4}/Mg_{5.52}Al_2O_{8.52}$.

Table 2
Hydrogenolysis of glycerol on $Pd_xCu_{0.4}/Mg_{5.6-x}Al_2O_{8.6-x}$.[a]

Catalyst (%)	Solvent	Conversion (%)	Activity of exposed Cu (mol-glycerol/(mol-Cu h))[b]	Selectivity (%)		
				1,2-PDO	EG[c]	Others[d]
$Cu_{0.4}/Mg_{5.6}Al_2O_{8.6}$	H_2O	56.7	7.5	97.1	1.1	1.8
$Pd_{0.008}Cu_{0.4}/Mg_{5.592}Al_2O_{8.592}$	H_2O	59.1	5.8	96.8	2.5	0.7
$Pd_{0.024}Cu_{0.4}/Mg_{5.576}Al_2O_{8.576}$	H_2O	70.5	12.6	97.9	1.1	1.0
$Pd_{0.04}Cu_{0.4}/Mg_{5.56}Al_2O_{8.56}$	H_2O	76.9	9.7	97.2	1.6	1.2
$Pd_{0.08}Cu_{0.4}/Mg_{5.52}Al_2O_{8.52}$	H_2O	66.6	18.1	97.5	1.5	1.0
$Pd_{0.04}/Mg_{5.56}Al_2O_{8.56}$	H_2O	1.2	–	79.9	1.2	18.9
$Pd_{0.04}Cu_{0.4}/Mg_{5.56}Al_2O_{8.56}$	CH_3OH	89.5	11.2	98.2	1.7	0.1
$Pd_{0.04}Cu_{0.4}/Mg_{5.56}Al_2O_{8.56}$	C_2H_5OH	88.0	11.0	99.6	0.2	0.2

[a] Reaction conditions: 75 wt% solutions of glycerol 8.0 g, 2.0 MPa H_2, 180 °C, 10 h. The catalysts have been reduced under H_2 for 1 h.
[b] Defined as (mol of converted glycerol)/(mol of exposed Cu atom)/(reaction time, h).
[c] Ethylene glycol.
[d] Methanol, ethanol and 1-propanol.

Table 3
Hydrogenolysis of glycerol over different amounts of $Pd_{0.04}Cu_{0.4}/Mg_{5.56}Al_2O_{8.56}$ in aqueous solution.[a]

Catalyst weight (g)	Conversion (%)	Activity of exposed Cu (mol-glycerol/(mol-Cu h))[b]	Selectivity (%)		
			1,2-PDO	EG[c]	Others[d]
0.25	24.7	12.4	97.8	1.3	0.9
0.5	48.7	12.2	97.6	1.6	0.8
1.0	76.9	9.7	97.2	1.6	1.2
1.5	91.2	7.6	97.0	1.7	1.3

[a] Reaction conditions: 75 wt% aqueous solutions of glycerol 8.0 g, 2.0 MPa H_2, 180 °C, 10 h.
[b] Defined as (mol of converted glycerol)/(mol of exposed Cu atom)/(reaction time, h).
[c] Ethylene glycol.
[d] Methanol, ethanol and 1-propanol.

three obvious H_2 desorption peaks (at 90–140, 240–300 and 300–360 °C) appeared in $Pd_{0.024}Cu_{0.4}/Mg_{5.576}Al_2O_{8.576}$ (curve c in Fig. 7). And these peaks enhanced in $Pd_{0.04}Cu_{0.4}/Mg_{5.56}Al_2O_{8.56}$ (curve d in Fig. 7) and $Pd_{0.08}Cu_{0.4}/Mg_{5.52}Al_2O_{8.52}$ (curve e in Fig. 7). These results indicated that the addition of Pd contributed to the ability of adsorbing hydrogen. According to those published works in this area [49–52], the resolved peak at low temperature (90–140 °C) could be ascribable to the decomposition of PdH_x or
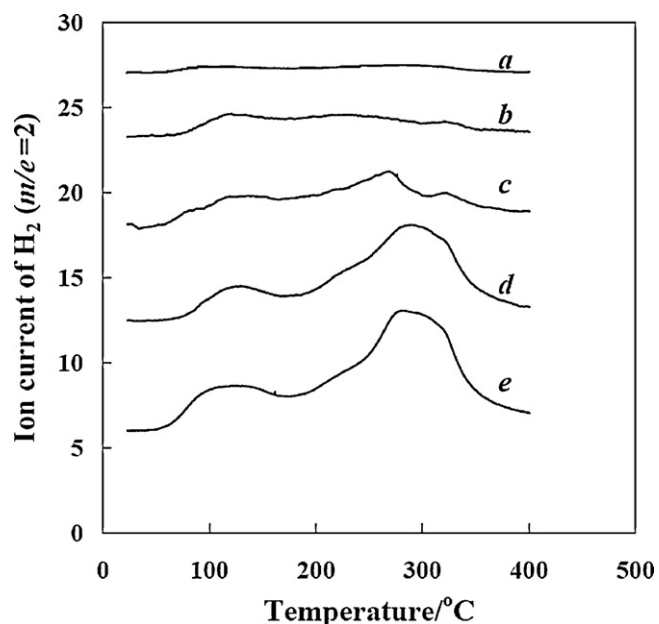

Fig. 7. H_2-TPD profile of the reduced catalysts. (a) $Cu_{0.4}/Mg_{5.6}Al_2O_{8.6}$; (b) $Pd_{0.008}Cu_{0.4}/Mg_{5.592}Al_2O_{8.592}$; (c) $Pd_{0.024}Cu_{0.4}/Mg_{5.576}Al_2O_{8.576}$; (d) $Pd_{0.04}Cu_{0.4}/Mg_{5.56}Al_2O_{8.56}$; (e) $Pd_{0.08}Cu_{0.4}/Mg_{5.52}Al_2O_{8.52}$.

hydrogen adsorbed on Pd. While a much broader signal in the range of 240–300 °C monitors the desorption of hydrogen from Cu particles, and the shoulder peak at 300–360 °C would arise from the split H–H on the surface of Mg–Al–O oxides [57–60]. These results suggested that hydrogen activation and spillover phenomena driven by the added Pd markedly influence the adsorption of H_2 and also contributed to the non-stoichiometric H_2 consumption in H_2-TPR profile (see Section 3.3 and Fig. 3). And these enhanced H_2 activation ability would improve its activity for glycerol hydrogenolysis.

3.8. Hydrogenolysis of glycerol over $Pd_xCu_{0.4}/Mg_{5.6-x}Al_2O_{8.6-x}$

Table 2 summarized the activity of $Pd_xCu_{0.4}/Mg_{5.6-x}Al_2O_{8.6-x}$ catalysts for hydrogenolysis of glycerol at 180 °C in aqueous solution. At low hydrogen pressure (2.0 MPa) and short time (10 h), the conversion of glycerol and the selectivity of 1,2-PDO on $Cu_{0.4}/Mg_{5.6}Al_2O_{8.6}$ were 56.7% and 97.1%, respectively. It is interesting to note that the conversion of glycerol increased first with the amount of added Pd in $Pd_xCu_{0.4}/Mg_{5.6-x}Al_2O_{8.6-x}$ catalysts. $Pd_{0.04}Cu_{0.4}/Mg_{5.56}Al_2O_{8.56}$ has the highest conversion of glycerol (76.9%) and a 97.2% 1,2-PDO selectivity. But the conversion of glycerol decreased to 66.6% on $Pd_{0.08}Cu_{0.4}/Mg_{5.52}Al_2O_{8.52}$ and this can be ascribed to that the surface area of this sample is low (154.8 m^2/g, see Table 1), the dispersion of Cu is poor and separated Pd particles formed (see the TEM image in Fig. 5e). As a reference, $Pd_{0.04}/Mg_{5.56}Al_2O_{8.56}$ was also prepared in the same procedure as $Pd_xCu_{0.4}/Mg_{5.6-x}Al_2O_{8.6-x}$ and used in hydrogenolysis of glycerol. But the conversion of glycerol on $Pd_{0.04}/Mg_{5.56}Al_2O_{8.56}$ was quite low (1.2%). The activity of per exposed Cu atom was calculated ((mol of converted glycerol)/(mol of exposed Cu atom)/(reaction time, h)) and summarized in Table 2. Compared with these published works of hydrogenolysis of glycerol in liquid phase [13–16,31–38,43–45], the reaction temperature (180 °C) of this work is low and the H_2

Table 4
Hydrogenolysis of glycerol on $Pd_{0.04}Cu_{0.4}/Mg_{5.56}Al_2O_{8.56}$ at different temperatures and recycled catalyst.[a]

Temperature (°C)	Conversion (%)	Activity of exposed Cu $(mol_{-glycerol}/(mol_{-Cu}\ h))$[b]	Selectivity (%)			
			1,2-PDO	2-Hydroxyacrolein	EG[c]	Others[d]
120	10.4	1.3	96.0	3.0	0	1.0
150	30.8	3.9	99.3	0.2	0	0.5
180	76.9	9.7	97.2	0.2	1.6	1.0
200	95.0	11.9	96.1	0.1	2.6	1.2
180[e]	50.0	6.1	97.9	0.0	2.0	0.1

[a] Reaction conditions: 75 wt% aqueous solutions of glycerol 8.0 g, 2.0 MPa H_2, 1.0 g reduced catalyst, 10 h.
[b] Defined as (mol of converted glycerol)/(mol of exposed Cu atom)/(reaction time, h).
[c] Ethylene glycol.
[d] Methanol, ethanol and 1-propanol.
[e] Five-times recycled catalyst.

pressure is the lowest (2.0 MPa). The activity of Cu in this work is higher than that of Pt/MgO [36], Cu/MgO [37], Cu/LDH [38], Cu/ZnO [45], and Pt/TiO$_2$ [44]. These results indicated Pd in bimetallic Pd-Cu/solid-base catalysts enhanced the activity of mono-metallic Cu/solid-base and there is a synergistic effect between Pd and Cu.

It was popularly accepted that the acid and basic sites in the catalysts play a key role on the hydrogenolysis mechanism of glycerol and a series of alcohols [3,17–42,61], and the influence of the acidity of $Pd_xCu_{0.4}/Mg_{5.6-x}Al_2O_{8.6-x}$ catalysts cannot be neglected in these researches. In this work, the acidity and basicity of $Pd_xCu_{0.4}/Mg_{5.6-x}Al_2O_{8.6-x}$ catalysts were detected by NH$_3$-TPD (Fig. 6A) and CO$_2$-TPD (Fig. 6B), it was found that these properties changed slightly after the addition of Pd. At the same time, the addition of Pd decreased the surface area of $Pd_xCu_{0.4}/Mg_{5.6-x}Al_2O_{8.6-x}$ and the dispersion of copper changed slightly. These results inferred that the increased hydrogenolysis ability of $Pd_xCu_{0.4}/Mg_{5.6-x}Al_2O_{8.6-x}$ catalysts cannot be explained by a modification of copper dispersion or the acidity of catalyst associated with the incorporation of Pd. At the same time, the low activity of mono-metallic $Pd_{0.04}/Mg_{5.56}Al_2O_{8.56}$ also indicated that the enhanced activity is not due to additional Pd sites, but to a synergetic effect of Pd on the active Cu sites. H$_2$-TPR experiments observed that the reduction of copper in bimetallic Pd-Cu/solid-base catalyst was improved obviously (Fig. 3) and Pd could provide a high concentration of active hydrogen. H$_2$-TPD experiments further confirmed that the hydrogen activation and spillover phenomena driven by the added Pd markedly influence the adsorption of H$_2$. These discussions could be concluded in that the hydrogenolysis of glycerol over $Pd_xCu_{0.4}/Mg_{5.6-x}Al_2O_{8.6-x}$ catalysts would perform in a consecutive dehydrogenation–dehydration–hydrogenation mechanism as that reported in base solutions (see Scheme 2) [31–42]. And the achievement of this work is that we found that the bimetallic Pd-Cu (hydrogenation center in Scheme 2) is more active than that of separated Cu and Pd because of H$_2$-spillover from Pd to Cu (see Scheme 3).

The hydrogenolysis of glycerol over $Pd_{0.04}Cu_{0.4}/Mg_{5.56}Al_2O_{8.56}$ was also performed in the solution of methanol and ethanol. It can be found that the conversion of glycerol reached 89.5 and 88.0%, respectively, when methanol and ethanol were used as solvent. And the selectivity of 1,2-PDO reached 99.6% in ethanol solution. These results could be ascribed to that the adsorption of water on the surface of catalyst is stronger than that of methanol and ethanol, which hindered the accessibility of glycerol [62].

### 3.9. Hydrogenolysis of glycerol with different amounts of catalyst in aqueous solution

Table 3 summarized the influence of different amount of added $Pd_{0.04}Cu_{0.4}/Mg_{5.56}Al_2O_{8.56}$ catalyst on glycerol hydrogenolysis at

180 °C and 2.0 MPa H$_2$. It can be found that the conversion of glycerol increased from 24.7 to 91.2% when the catalyst weight increased from 0.25 to 1.5 g, but the selectivity of 1,2-PDO changed slightly. These results confirmed that glycerol hydrogenolysis can perform on $Pd_{0.04}Cu_{0.4}/Mg_{5.56}Al_2O_{8.56}$ catalyst in a wide ranged amount of catalyst.

3.10. Hydrogenolysis of glycerol at different temperatures in aqueous solution

Table 4 summarized the results of hydrogenolysis of glycerol on $Pd_{0.04}Cu_{0.4}/Mg_{5.56}Al_2O_{8.56}$ catalyst at different temperatures. It can be found that glycerol hydrogenolysis accelerated with the increasing temperature. The conversion of glycerol increased quickly from 10.4 (at 120 °C) to 95.0% (at 200 °C), but the selectivity of 1,2-PDO passed it maximum (99.3%) at 150 °C. Intermediates (2-hydroxyacrolein, with a 3.0% selectivity) appeared at low temperature. These results indicated that this catalyst is more active and selective for glycerol hydrogenolysis towards 1,2-PDO and no obvious cleavage of C–C bond occurred even at high temperature. The high selectivity of 1,2-PDO could be attributed to that products diffused quickly in the mesopores of $Pd_{0.04}Cu_{0.4}/Mg_{5.56}Al_2O_{8.56}$ which restrained its secondary reactions.

At 180 °C, the catalyst was recycled simply by filtration. It can be found that the detected conversion of glycerol in 5th recycle decreased to 50.0%. In order to seek the reason of decreased glycerol conversion, actual composition of fresh catalyst and 5-recycled catalyst were checked (and summarized in Table S1 in the supplementary data). It can be concluded that the deactivation of bimetallic Pd-Cu/solid-base catalyst could be ascribed to the leaching of Cu. That is, improving the stability of active copper against leaching in polar reaction medium should be paid more attention in the future.
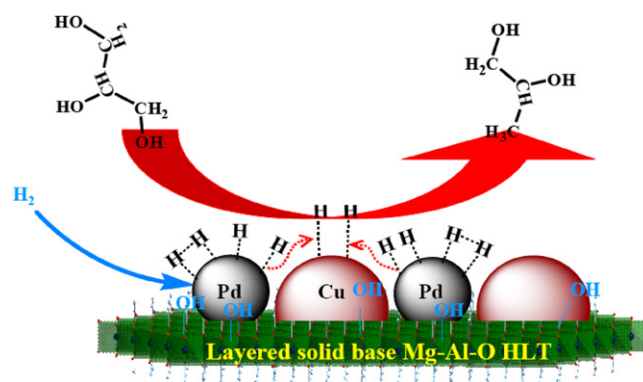
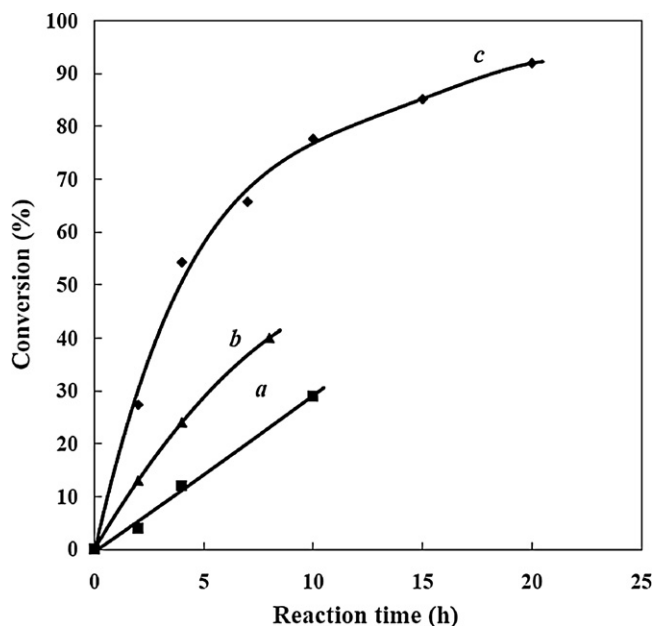**Scheme 3.** Glycerol hydrogenolysis on bimetallic Pd-Cu/solid-base catalyst.

Fig. 8. Time courses of glycerol hydrogenolysis over $Pd_{0.04}Cu_{0.4}/Mg_{5.56}Al_2O_{8.56}$. (a) 150 °C; (b) 160 °C; (c) 180 °C (reaction conditions: 75 wt% aqueous solution of glycerol 8.0 g, 1.0 g reduced catalyst 2.0 MPa H_2).

3.11. Kinetics of glycerol hydrogenolysis in aqueous solution

Fig. 8 shows the time courses of glycerol hydrogenolysis over $Pd_{0.04}Cu_{0.4}/Mg_{5.56}Al_2O_{8.56}$ catalyst at 180, 160 and 150 °C. At 180 °C, the conversion of glycerol increased quickly in the first 15 h, and then increased slowly from to 83.4 (at 15 h) to 90.2% (20 h), the selectivity of 1,2-PDO decreased slightly from 98.3 to 96.6%. These results indicated that the conversion of glycerol depended strongly on the concentration of the glycerol in reaction mixture. On the other hand, the detected conversion of glycerol increased linearly at lower reaction temperatures (160 and 150 °C) and the selectivity of 1,2-PDO remained higher than 98.5%.

According to these time courses at different temperatures, the relation between $\ln(c_{glycerol})$ and reaction time is found to be in linearly (see Fig. S4 in the supplementary data). And the calculated reaction rate constants are 0.0352, 0.0636 and 0.1527 h^{-1} at 150, 160, and 180 °C, respectively (see Fig. S4 and Table S2 in the supplementary data). According to these data, the calculated activation energy of glycerol hydrogenation over $Pd_{0.04}Cu_{0.4}/Mg_{5.56}Al_2O_{8.56}$ in the temperature range of 150–180 °C is 77.1 kJ mol^{-1} (see Table S2 in the supplementary data).

4. Conclusion

In summary, this work confirmed that bimetallic Pd-Cu/solid-base catalysts could be prepared via thermal decomposition of layered double hydroxides precursors. And these $Pd_xCu_{0.4}/Mg_{5.6-x}Al_2O_{8.6-x}$ catalysts are effective in hydrogenolysis of glycerol to 1,2-PDO at a wide ranged temperature and reaction time. The high performance of Pd-Cu/solid-base catalysts was attributed to the H_2-spillover from Pd to Cu.

Acknowledgment

Appendix A. Supplementary data

Supplementary data associated with this article can be found, in the online version, at doi:10.1016/j.apcata.2011.06.026.

References

[1] D.R. Dodds, R.A. Grsoo, Science 318 (2007) 1250–1251.
[2] B. Katryniok, S. Paul, V. Bellière-Baca, P. Rey, F. Dumeignil, Green Chem. 12 (2010) 2079–2098.
[3] B.N. Zope, D.D. Hibbitts, M. Neurock, R.J. Davis, Science 330 (2010) 74–78.
[4] A. Villa, G.M. Veith, L. Prati, Angew. Chem. Int. Ed. 49 (2010) 4499–4502.
[5] A. Villa, A. Gaiassi, I. Rossetti, C.L. Bianchi, K. Benthem, G.M. Veith, L. Prati, J. Catal. 275 (2010) 108–116.
[6] D. Liang, J. Gao, J.H. Wang, P. Chen, Z.Y. Hou, X.M. Zheng, Catal. Commun. 10 (2009) 1586–1590.
[7] S.H. Chai, H.P. Wang, Y. Liang, B.Q. Xu, Green Chem. 9 (2007) 1130–1136.
[8] F. Cavani, S. Guidetti, L. Marinelli, M. Piccinini, E. Ghedini, M. Signoretto, Appl. Catal. B 100 (2010) 197–204.
[9] F. Wang, J.L. Dubois, W. Ueda, J. Catal. 268 (2009) 260–267.
[10] B. Katryniok, S. Paul, M. Capron, C. Lancelot, V. Bellière-Baca, P. Rey, F. Dumeignil, Green Chem. 12 (2010) 1922–1925.
[11] I. Gandarias, P.L. Arias, J. Requies, M.B. Güemez, J.L.G. Fierro, Appl. Catal. B 97 (2010) 248–256.
[12] J. Chaminand, L. Djakovitch, P. Gallezot, P. Marion, C. Pinel, C. Rosier, Green Chem. 6 (2004) 359–361.
[13] T. Miyazawa, Y. Kusunoki, K. Kunimori, K. Tomishige, J. Catal. 240 (2006) 213–221.
[14] T. Miyazawa, S. Koso, K. Kunimori, K. Tomishige, Appl. Catal. A 318 (2007) 244–251.
[15] E.S. Vasiliadou, E. Heracleous, I.A. Vasalos, A.A. Lemonidou, Appl. Catal. B 92 (2009) 90–99.
[16] Y. Shinmi, S. Koso, T. Kubota, Y. Nakagawa, K. Tomishige, Appl. Catal. B 94 (2010) 318–326.
[17] J. Macht, C.D. Baertsch, M. May-Lozano, S.L. Soled, Y. Wang, E. Iglesia, J. Catal. 227 (2004) 479–491.
[18] F. Wang, W. Ueda, Catal. Today 144 (2009) 358–361.
[19] N.M. Bertero, A.F. Trasarti, C.R. Apesteguia, A.J. Marchi, Appl. Catal. A 394 (2011) 228–238.
[20] N.M. Bertero, C.R. Apesteguía, A.J. Marchi, Catal. Commun. 10 (2008) 261–265.
[21] J. Deleplanque, J.-L. Dubois, J.-F. Devaux, W. Ueda, Catal. Today 157 (2010) 351–358.
[22] A.J. Marchi, D.A. Gordo, A.F. Trasarti, C.R. Apesteguía, Appl. Catal. A 249 (2003) 53–67.
[23] N.M. Bertero, C.R. Apesteguía, A.J. Marchi, Catal. Commun. 10 (2009) 1339–1344.
[24] F. Wang, W. Ueda, Appl. Catal. A 346 (2008) 155–163.
[25] N.M. Bertero, C.R. Apesteguía, A.J. Marchi, Appl. Catal. A 349 (2008) 100–109.
[26] F. Wang, J.-L. Dubois, W. Ueda, J. Catal. 268 (2009) 260–267.
[27] F. Wang, J.-L. Dubois, W. Ueda, Appl. Catal. A 376 (2010) 25–32.
[28] C.D. Baertsch, K.T. Komala, Y.-H. Chua, E. Iglesia, J. Catal. 205 (2002) 44–57.
[29] F. Arena, G. Italiano, K. Barbera, S. Bordiga, G. Bonura, Appl. Catal. A 350 (2008) 16–23.
[30] M.C.N. Amorim de Carvalho, F.B. Passos, M. Schmal, Catal. Commun. 3 (2002) 503–509.
[31] E.P. Maris, R.J. Davis, J. Catal. 249 (2007) 328–337.
[32] E.P. Maris, W.C. Ketchie, M. Murayama, R.J. Davis, J. Catal. 251 (2007) 281–294.
[33] M. Pagliaro, R. Ciriminna, H. Kimura, M. Rossi, C.D. Pina, Angew. Chem. Int. Ed. 46 (2007) 4434–4440.
[34] A. Behr, J. Eilting, K. Irawadi, J. Leschinski, F. Lindner, Green Chem. 10 (2008) 13–30.
[35] C.W. Chiu, M.A. Dasari, W.R. Sutterlin, G.J. Suppes, Ind. Eng. Chem. Res. 45 (2006) 791–795.
[36] Z.L. Yuan, P. Wu, J. Gao, X.Y. Lu, Z.Y. Hou, X.M. Zheng, Catal. Lett. 130 (2009) 261–265.
[37] Z.L. Yuan, J.H. Wang, L.N. Wang, W.H. Xie, P. Chen, Z.Y. Hou, X.M. Zheng, Bioresour. Technol. 101 (2010) 7088–7092.
[38] Z.L. Yuan, L.N. Wang, J.H. Wang, S.X. Xia, P. Chen, Z.Y. Hou, X.M. Zheng, Appl. Catal. B 101 (2011) 431–440.
[39] J.I. Di Cosimo, V.K. Díez, M. Xu, E. Iglesia, C.R. Apesteguía, J. Catal. 178 (1998) 499–510.
[40] V.K. Díez, C.R. Apesteguía, J.I. Di Cosimo, J. Catal. 240 (2006) 235–244.
[41] J.I. Di Cosimo, C.R. Apesteguía, M.J.L. Ginés, E. Iglesia, J. Catal. 190 (2000) 261–275.
[42] C.A. Ferretti, A. Soldano, C.R. Apesteguia, J.I. Di Cosimo, Chem. Eng. J. 161 (2010) 346–354.
[43] A. Alhanash, E.E. Kozhevnikova, I.V. Kozhevnikov, Catal. Lett. 120 (2008) 307–311.
[44] J. Feng, J. Wang, Y. Zhou, H. Fu, H. Chen, X. Li, Chem. Lett. 36 (2007) 1274–1278.
[45] S. Wang, H. Liu, Catal. Lett. 117 (2007) 62–67.

[46] C.J.G. Van Der Grift, A.F.H. Wielers, B.P.J. Jogh, J. Van Beunum, M. De Boer, M. Versluijs-Helder, J.W. Geus, J. Catal. 131 (1991) 178–189.
[47] A. Gervasini, S. Bennici, Appl. Catal. A 281 (2005) 199–205.
[48] S. Kannan, A. Dubey, H. Knozinger, J. Catal. 231 (2005) 381–392.
[49] I. Melián-Cabrera, M.L. Granados, J.L.G. Fierro, J. Catal. 210 (2002) 285–294.
[50] I. Melián-Cabrera, M.L. Granados, J.L.G. Fierro, J. Catal. 210 (2002) 273–284.
[51] O.M. Iiinich, E.N. Gribov, P.A. Simonov, Catal. Today 82 (2003) 49–56.
[52] D.R. Luebke, L.S. Vadlamannati, V.I. Kovalchuk, J.L. d'Itri, Appl. Catal. B 35 (2002) 211–217.
[53] J.H. Fei, Z.Y. Hou, B. Zhu, H. Lou, X.M. Zheng, Appl. Catal. A 304 (2006) 49–54.
[54] D.F. Jin, B. Zhu, Z.Y. Hou, J.H. Fei, H. Lou, X.M. Zheng, Fuel 86 (2007) 2707–2713.
[55] R. Anand, R. Maheswari, K.U. Gore, S.S. Khaire, V.R. Chumbhale, Appl. Catal. A 249 (2003) 265–274.
[56] J. Gao, J.Z. Guo, D. Liang, Z.Y. Hou, J.H. Fei, X.M. Zheng, Int. J. Hydrogen Energy 33 (2008) 5493–5500.
[57] J.A. Ahlers, J.A. Grasser, B.T. Loveless, D.S. Muggli, Catal. Lett. 114 (2007) 185–191.
[58] H. Wilmer, T. Genger, O. Hinrichesen, J. Catal. 215 (2003) 188–198.
[59] T. Genger, O. Hinrichsen, M. Muhker, Catal. Lett. 59 (1999) 137–141.
[60] F. Arena, G. Italiano, K. Barbera, S. Bordiga, G. Bonura, L. Spadaro, F. Frusteri, Appl. Catal. A 350 (2008) 16–23.
[61] C.A. Ferretti, C.R. Apesteguía, J.I. Di Cosimo, Appl. Catal. A 399 (2011) 146–153.
[62] A. Bienholz, F. Schwab, P. Claus, Green Chem. 12 (2010) 290–295.